A.V.Moiseev, V.L. Afanasiev, S.N. Dodonov

Special Astrophysical Observatory , Nizhnij Arkhyz, Karachaevo-Cherkesia, 357147, Russia

V.V. Mustsevoi and S.S. Khrapov

Volgograd State University, Volgograd, 400062, Russia

Abstract

2D spectral observations for 4 Sy galaxies with ionization cones are presented. Images in the [OIII] line, velocity fields of the ionized gas, stellar velocity and dispersion fields were obtained at the SAO RAS 6m telescope. Non-circular gaseous motions and Z-shaped emission filaments may be explained as helical waves which located in the ionization cone. This waves are generated by the hydrodynamical instability due to the velocity break between galactic ISM and outflowing from the AGN engine. The axis of cone lies slightly align with direction of a nuclear mini bar.

1 Introduction

A lot of Narrow Line Regions (NLRs) in the Seyfert galaxies have a cone-like morphology. In this work we discussed the structure of galaxies with following observational features:

- an axis of cone lies near with direction of a radio jet (Wilson&Tsevetanov,1994);
- a multicomponent structure of the narrow emission lines ([OIII] as example) shows that some systems of the gaseous clouds existed (include high-velocities ($100 \div 1000\,\mathrm{km\,s^{-1}}$) radial outflow motions);
- emission filaments have a Z(S)-shaped or/and arcs-like ("strands") structure;
- large gradients of the line-of-sight gaseous velocities into Z-shaped spiral exist, also a different location of "blue" and "red" components of the emission lines presents on the sky-plane in different parts of the Z-shaped structure.

As example we considered the galaxies Mrk 3, Mrk 573, NGC 3516 and NGC 5252. For each object some models were proposed in references. These are complex of inclined and polar gaseous discs in NGC 5252 (Morse et al.,1998) and in Mrk 3 (Afanasiev & Sil'chenko, 1990), bent bipolar outflow or precessed jet for NGC 3516 (Veilleux et al.,1993). But such kind of structures is unstable and has short live-time, or the very specific orientation in relative to Earth observer is need, or an unusual power is required (for jet precessing on scale ~ 3 Kpc). Recently model of jet-cloud interaction for Mrk 3 (Rossi et al.,2000), cannot descibe a Z-shaped emission pattern in NLR.

2 The hypothesis.

In the first place, we propose that observable Z-shaped structures of NLRs are **tridimensional helical waves** into the ionizations cone. These waves generated by the hydrodynamical instability due the velocity break between galactic ISM and a central outflowing. A collimated radio jet associated with direction of outflow and matches with the cone's axis.

In the second place, we considered the **orientation of the cone**. The Unified Model of AGN assuming the presence of circumnuclear disk (torus) around the central engine which collimates a jet outflow and ionized radiation. We propose that torus orientation associated with **a particular directions** in a galactic body. In an easy axisymmetrical case this is direction of the rotation axis. All galaxies from our sample have a triaxial structures in central regions (Mrk 573 and NGC 3516 are double-barred galaxies, Mrk 3 and NGC 5252 have a probable central mini bar, see section 3.1, 3.4). In triaxial gravity potential, there are three planes where stable orbit is possible: this planes are lying along its axis. Let us note that most stable orbits are located in the smaller dimensional plane, i.e. rotation matter has a minimal angular moment. The gas in a galactic disk decelerates by bar and accumulates to the torus. A resulting radiation and outflowing cone will coincide with the angular momentum vector of the torus [1] (near by a major axis of a cental bar).

3 Observations

The observations with Interferometer Fabry-Perot (IFP) were done at the SAO RAS 6m telescope in 1996-1998. A [OIII]λ5007 line contain in a spectral range, a spectral resolution $40-100\,\mathrm{km\,s^{-1}}$, a spatial resolution $1''.5$-$2''$. Mkn 3 and NGC 5252 were observed with integral field spectrograph MPFS in 1999-2000. Spectral ranges are $\lambda 4900-6100\mathring{A}$, $\lambda 4000-5200\mathring{A}$, spectral resolution is $120-150\,\mathrm{km\,s^{-1}}$, spatial data sampling is $1''$/lens in $16''\times 15''$ field-of-view. The stellar velocity and dispersion fields were obtained from the absorptions spectra analysis (Tonry&Davis,1979). For Mrk 573 and NGC 3516 we take the previous MPFS-data (Afanasiev et al.,1995; Afanasiev&Vlasyuk,1995) with similar spectral and spatial resolutions.

We fit by hand the observable Z-shaped emission arms in easy assumption of a helical log-scale spiral on a surface of a cone. The axis of cone was setting near by the galactic plane and projected on the sky-plane in alignment with radio jet direction. The fitting results are overlapping on [OIII] images and velocity fields (Fig. 1-4)

In a helix assumption the mutlicomponent structure of emission line will be presented when blueshift and redshift parts of the helical spiral lie along a line-of-sight. This fact also was taken into consideration.

3.1 Mrk 3 (S0, Seyfert 2)

The NLR has a bi-conical structure which extended more than $8''$ (2 kpc), elongated in $PA=114^o$ (Pogge&De Robertic,1993) and shows a Z-shaped structure on HST-images (see Fig. 1a and Capetti et al., 1995). The analysis of the stellar velocity field shows that PA of a kinematical major axis shifted on 7^o relative the photometrical $PA=23^o$ in $r<6''$. This discrepancy relates with a oval orbit distortion due to the large-scale bar with $a\sim 20''$. We fit the HST image with 2D model (oblate spheroid+disk+Ferrer's bar, Fig. 1b). A small-scale bar may be also presents in the galaxy (Capetti et al., 1995) with $r\leq 1''$ and $PA\approx 70^o$.

The profiles of the [OIII] line in IFP-data demonstrate a multicomponent structure (Fig. 1c) in agreement with long-slit data by Afansiev&Sil'chenko(1990). The distance between components is $100-500\,\mathrm{km\,s^{-1}}$. A kinematical axis in the velocity field of main (brightest) component turns away from the stellar axis more than $\sim 80^o-120^o$. A velocity gradient along the helical spiral is presented in $r<7''$. The second component of the [OIII] also shows non-circular motions, located only in the helical structure and has inverse velocities in comparison

[1] Axon & Robinson(1996) and Vila-Vilaro (1995) also argued that torus due the vertical inner ILR into a secondary bar and alignment with its direction.

with the main component (Fig. 1d). In $r < 5''$ the third (low-brightness) component of the [OIII] line is presented and corresponds to the stellar motions into the large-scale bar.

From the helical fitting we obtained an estimation on the ionized cone open angle $\theta_0 = 64^o$, and the inclination angle to the galaxy plane $\delta i < 10^o$.

3.2 Mrk 573 (SAB0, Seyfert 2)

The NLR elongated in $PA \approx 120^o$ and extended at $\sim 13''$ (4.2 kpc, Wilson&Tsvetanov,1994). That shows an arc-like and Z-shaped bi-conical structures on ground-base and HST emission line images (Fig. 2a and Ferruit et al.,1999). The optical image of the galaxy can be fitted in double-barred assumption with lengths of bars $5''$ and $20''$ (Fig. 2b, and Moiseev,1998). The secondary bar ($PA \approx 115^o$) distorts the stellar velocity field (Fig. 2e) in $r < 5''$. The [OIII] line in $r < 6''$ has a double-component profile (Fig. 2c) with separation $\pm 200\,\mathrm{km\,s^{-1}}$ in agreements with preview 2D spectroscopy investigations (Afanasiev et al. 1995). The main component shows the strong non-circular motions with $100 - 200\,\mathrm{km\,s^{-1}}$ in amplitude. The second component located along the cone's axis and demonstrated an invert sign of the velocities (Fig. 2d). Note that Ferruit et al.(1999) carried out the a 2D spectroscopy of the galaxy and found the strong red (blue) wings of the [OIII] line profile on distance $\pm 2 - 3''$ from the nucleus. In our IFP data these components are certainly decoupled (Fig. 2c).

From the helical fitting we obtained an estimation on cone open angle $\theta_0 = 56^o$, the inclination angle to the galaxy plane $\delta i \sim 0^o$. The axis of cones slightly align with a secondary bar major axis.

3.3 NGC 3516 (SB0, Seyfert 1.5)

The image in [OIII] line shows the broad cones in $PA = 52^o$ (Fig. 3a). The NLR extended on $\sim 38''$ (6.2 kpc) in NE and on $\sim 14''$(2.3 kpc) in SW directions in agreement with Miyaji et al.(1992). The emission regions on $r < 10''$ have a Z-shaped morphology, also available in HST data by Ferruit et.al(1998). We fit the continuum image of NGC 3516 with a double-barred model, where bars have sizes $6''$ and $22''$ (Fig. 3b). The central mini-bar has $PA \approx 55^o$ and matches with line-of-nodes of the stellar velocity field from Arribas et al.(1997) and with our MPFS-data. A double-component structure of the [OIII] profile (Fig. 3c and 3d), firstly pointed out by Mulchaey et al.(1992) is seen in $r < 10''$. The velocities of the emission components have a "blue-red" switch along the Z-shaped structure, in agreement with observations by Afanasiev et al. at the 4m Mayall telescope. On $r > 20''$ the line-of-sight velocities have a gradient across the cone axis (along the helical spiral arm).

From the helical fitting we obtained an estimation on cone open angle $\theta_0 = 60^o$, the inclination angle to the galaxy plane $\delta i < 5^o$. The axis of cones slightly align with a secondary bar major axis.

3.4 NGC 5252 (S0, Seyfert 1.9)

A beautiful bi-cone emission structure is extending in this galaxy more than $50''$ (~ 20 kpc). The central Z-shaped arms and outer arcs are revealed on the [OIII] image (Fig. 4a. and Morse et al.,1998). The major axis of J-band image (Alonso-Herrero et al.,1998) has $PA \approx 18^o$ in agreements with stellar rotation (Fig. 4a and 4d). We fitted the J-image with a axisymmetrical model (disk+oblate bulge) but the structure of the central isophotes is uncertain. The asymmetry in stellar dispersion field and "boxy" isophotes support of possible mini bar ($r < 5''$) existence but it puzzle into a high inclined disk. The second component of the [OIII] line profile is presented in $r < 7''$ (Fig. 4a-c). Partly it has circular (as stellar) rotation, strong non-circular motions also available. The velocity filed of the bright [OIII] component has a very strange structure (Fig. 4b): isovelocities turned across the galactic major axis in the central region and have an insignificant gradient at the outer part of the galaxy (in the outer arcs). The gaseous light-of-sight velocities show large disagreements ($100 - 400\,\mathrm{km\,s^{-1}}$) with the stellar one.

Note that helical model matched with emission filaments (and its velocities) only on $r < 10 - 20''$. The outer emission arcs have a small gradient of line-of-sight velocity and probably has a axis-symmetrcial structure.

4 A numeric simulations

We just started sets of 2D and 3D hydrodynamical simulations of a conical jet with optically thin radiative cooling in the field of parabolic gravity potential. This simulations show that heavy damping of all acoustical modes and little influence on unstable Kelvin-Helmholtz surface modes are presented. The effect of radiative cooling on waveguide-resonance internal gravity modes is various, modes moving relative to the jet matter from the sourse being always damped, the growth of modes moving towards the sourse is faster then in adiabatic jet. Our analysis shows that surface Kelvin-Helmholtz modes and waveguid-resonance internal gravity body modes will be most effective at producing shock waves outside from the central outflow (radio jet). Moreover, this shocks move in the cone with rather large opening angle than initial jet. The intensity radiative cooling in these shocks **provide heating of the ambient medium and forming a ionized cone.**

Our simulation shows that axisymmetrical waves are growing slower than helical waves. So these waves can be observed at the **outer regions**. An amplitude of the helical modes decrease with radius (unlike from axisymmetrical modes). And nonlinear superposition of helical and axisymmetrical waves can give the structure which observed in the NGC 5252. Moreover, our simulation shows that line-of-sight gaseous velocities must be linear increasing with distance from center, in good agreements with observations.

The distribution of the model "luminosity" shows at the Fig. 4e and 4f (in arbitrary scale of length, jet running from (0,0) point). These first results support our scenario of formation of the Z-spahed and arc-like emisission structures in Seyfert galaxies.

We postulate that model of NLR which including the bar, radio jet, ionization cone and helical waves in the cone may be constructed from easy assumption, without special limitations on the origin of AGN central engine.

Acknowledgements. We would like to thank astronomers of the SAO – Alexander Burenkov, Irina Kostiuk, Alla Shapovalova and Valery Vlasyuk for assisting at the 6m telescope, Sergej Drabek and Eugene Gerasimenko for technical supporting of the observations and 6m telescope committee for allocating observing time. Also we are grateful to Viktor Levi for helpful discussions and to to Almudena Alonso-Herrero who provided the J-band image of NGC 5252.

References

Afanasiev, V.L., Burenkov, A.N., Shapovalova, A.I., Vlasyuk, V.V.,1996, in IAU Coll.157,Vol.91, 218
Afanasiev, V.L., Vlasyuk, V.V.,1995, in IAU Coll.149,Vol. 71, 266
Afanasiev, V.L. & Sil'chenko, O.K., 1991,Bull. SAO,33,104
Alonso-Herrero, A., Simpson, C., Ward, M.J., Wilson, A.S.,1998,ApJ,495,196
Arribas, S.,Mediavilla, E., Garsia-Lorenzo, B., Del Burgo, C., 1997,ApJ,490,227

Axon, D.J. & Robinson, A., 1996, in Nobel Symposium 98,223
Capetti, A., Macchetto, F., Axon, D.J., et al.,1995,ApJ,448,600
Ferruit, P., Wilson A.S., Falcke, H., et al.,1999, MNRAS,309,1
Ferruit, P., Wilson, A.S., Mulchaey, J.S.,1998, ApJ,509,646
Miyaji, T., Wilson, A.S., Perez-Fournon, I.,1992,ApJ,385,137
Moiseev, A.V., 1998, SAO RAS preprint, N 134/1
Morse, J. A., Cecil, G., Wilson, A.S., Tsvetanov, Z.I.,1998,ApJ,505,159
Mulchaey, J.S., Tsvetanov, Z., Wilson, A.S., Perez-Fournon, I.,1992,ApJ,394,91
Pogge, R.W. & De Robertic, M.M., 1993,ApJ,404,563
Rossi, P., Capetti, A., Bodo, G., et al.,2000,A&A,356,73
Tonry, J. & Davis, M.,1979,AJ,84,1511
Veilleux, S., Tully, R.B., Bland-Hawtorn, J., 1993,AJ,105,1318
Vila-Vilaro, B., Robinson, A., Perez, E., et al.,1995,A&A,302,58
Wilson, A.S. & Tsvetanov, Z.I.,1994,AJ,107,1227

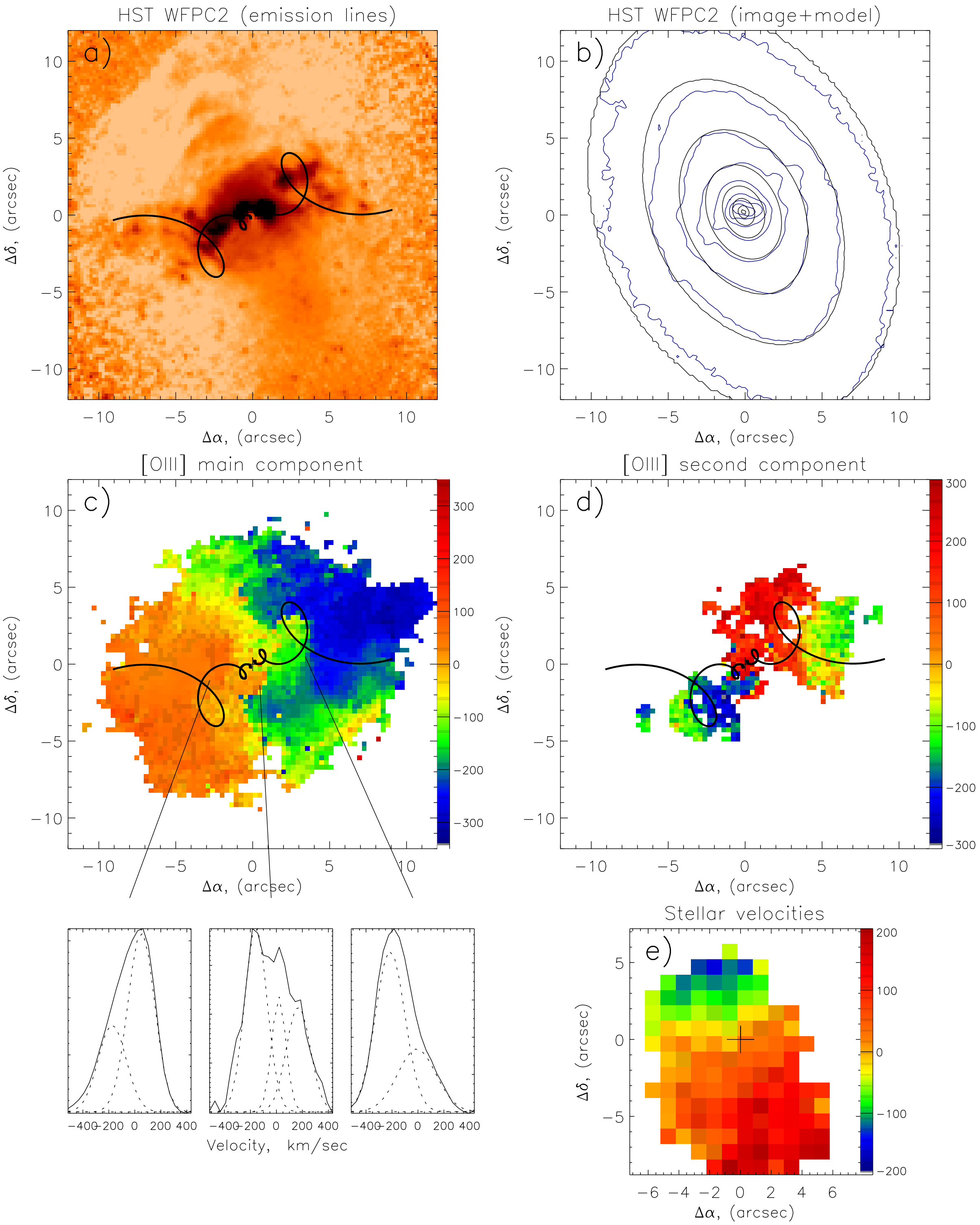

Figure 1: **Mrk 3, the Helical spiral are overlapping on the images.**. (a) Residual image after subtraction the 2D model of the continuum brightness from HST WFPC2 image in the filter F606 (HST data archive). The [OIII]λ5007, [OI]λ6300 and H_α emission lines has contribution into the residual image. (b) (blue) – HST WFP2 image; (black) – isophotes of the 2D model (oblate bulge+disc+ Ferrer's bar). (c) Velocity field of the main component of the [OIII] emission line. A color velocity scale – in $\mathrm{km\,s^{-1}}$ (in relative to system velocity $V_{SYS} = 4000\,\mathrm{km\,s^{-1}}$). Examples of the [OIII] emission line profile and gauss-decomposition of components show at the bottom panels. (d) Velocity field of the second component of [OIII]. (e) Stellar velocity field.

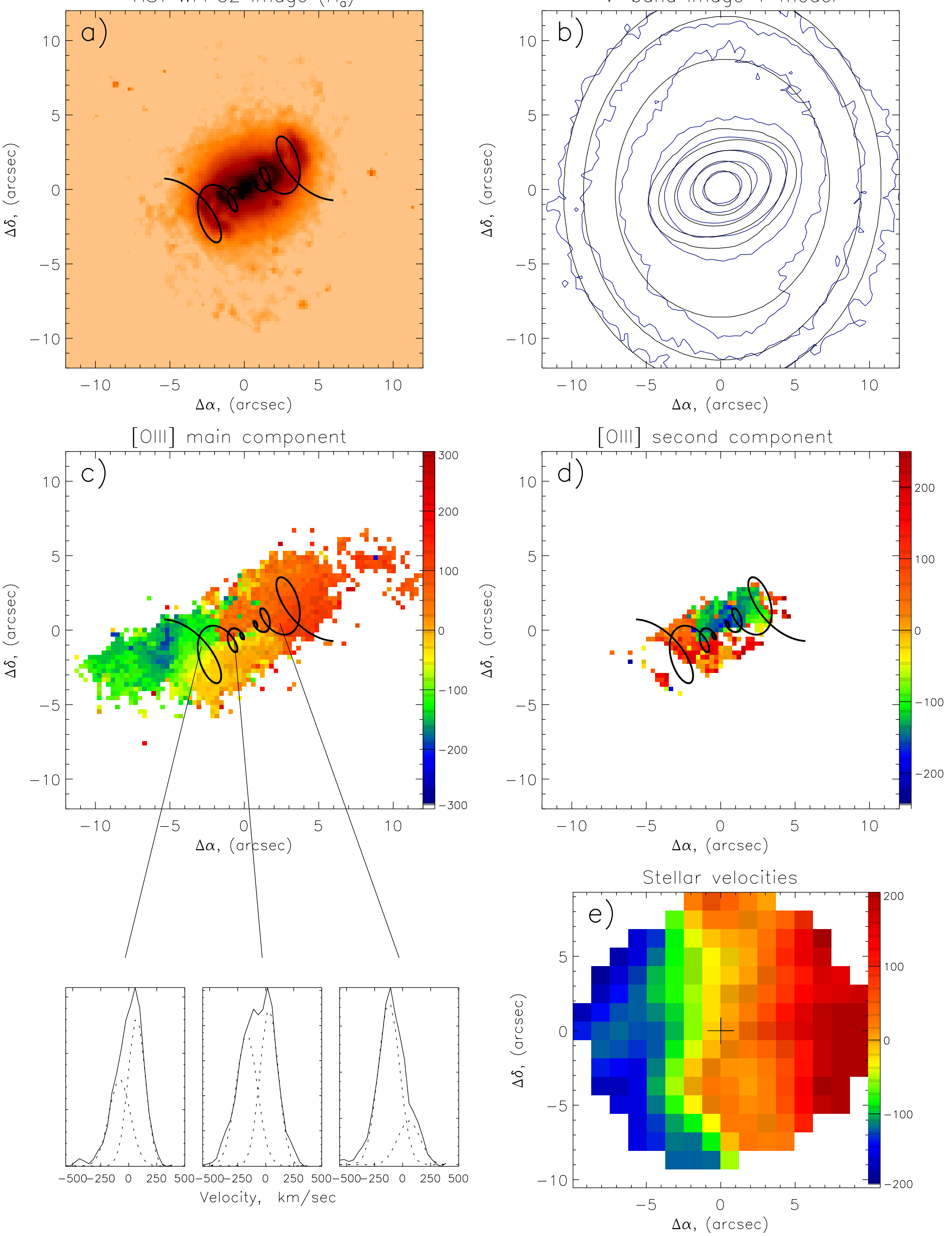

Figure 2: **Mrk 573, the Helical spiral are overlapping on the images.** (a) – HST WFPC2 image in the H_α emission line (filter FR680N, HST data archive). (b) (blue) – isophotes of the V-image (SAO RAS 1m telescope), (black) – isophotes of the 2D model (bulge+disc+two Ferrer's bars). (c) Velocity field of the main component of [OIII] ($V_{SYS} = 5160\,\mathrm{km\,s^{-1}}$). (d) Velocity field of the second component of [OIII]. (e) Stellar velocity field.

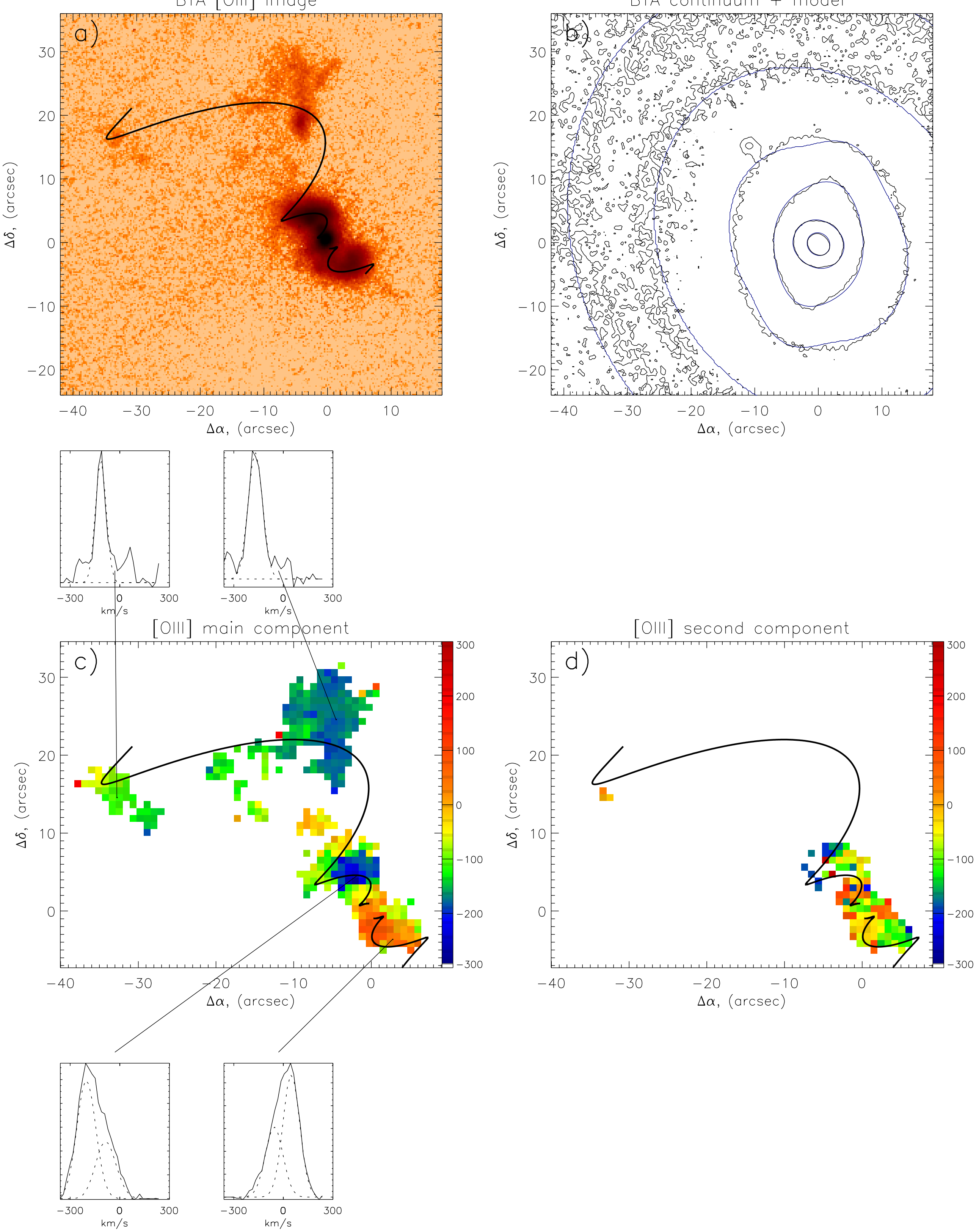

Figure 3: **NGC 3516, the Helical spiral are overlapping on the images.** (a) Image in the [OIII] emission line (6m telescope). (b) (blue) – continuum isophotes near [OIII]; (black) – isophotes of the 2D model (bulge+disc+two Ferrer's bars). (c) Velocity field of the main component of [OIII] ($V_{SYS} = 2560\,\mathrm{km\,s^{-1}}$). (d) Velocity filed of the second component of [OIII].

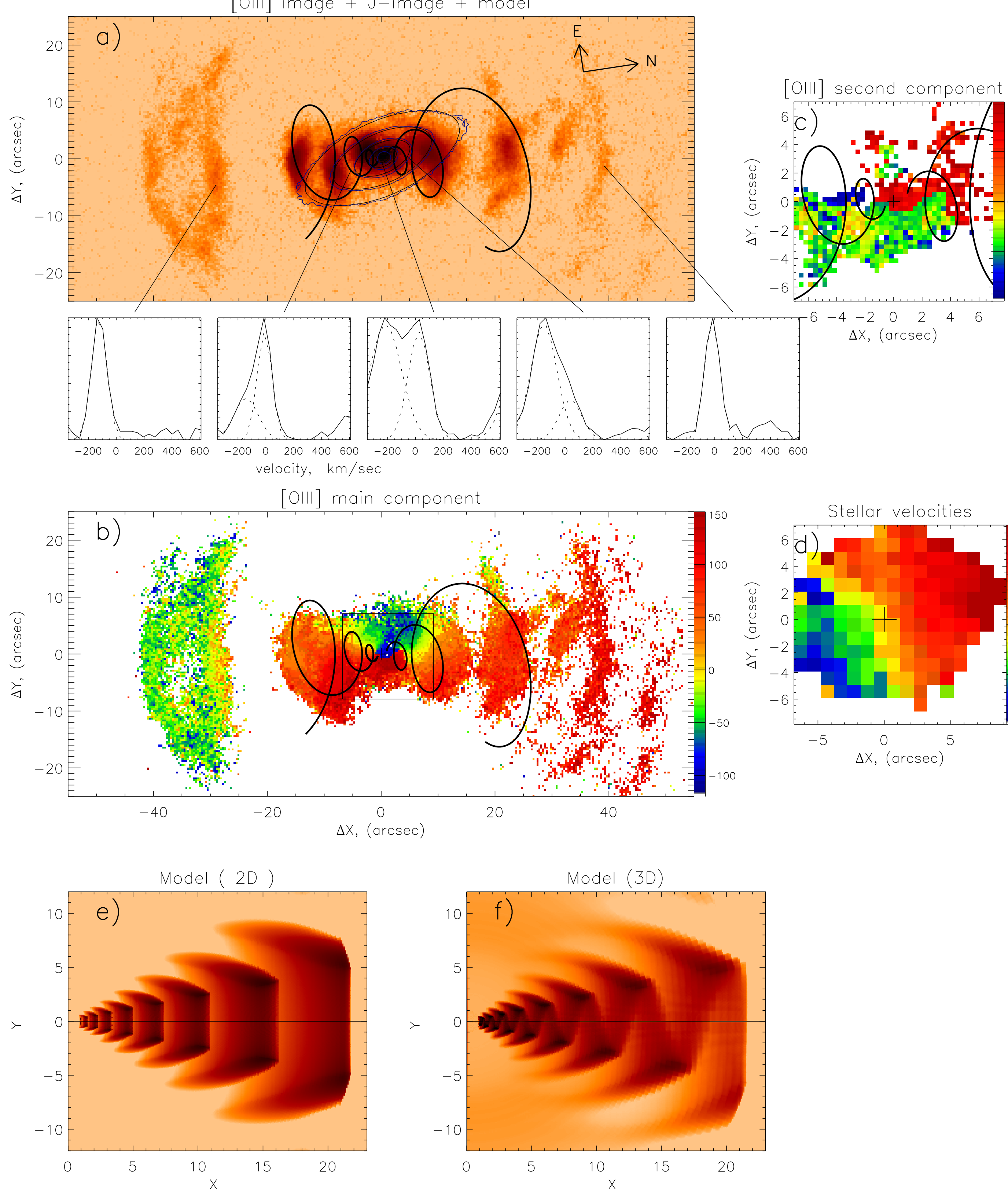

Figure 4: **NGC 5252, the Helical spiral are overlapping on the images.** (a) Image in the [OIII] emission line (IFP-data). Blue – isophotes of the J-band image, black – isophotes of the 2D model (bulge+disc) (b) Velocity field of the main component of [OIII] ($V_{SYS} = 6880\,\mathrm{km\,s^{-1}}$). (c) Velocity field of the second component of [OIII]. (d) Stellar velocity field. **Results of the simulations:** projection of the model luminosity on the "sky-plane". (e) axisymmetrical waves ("arcs"). (f) non-axisymmetrical waves ("helicon").

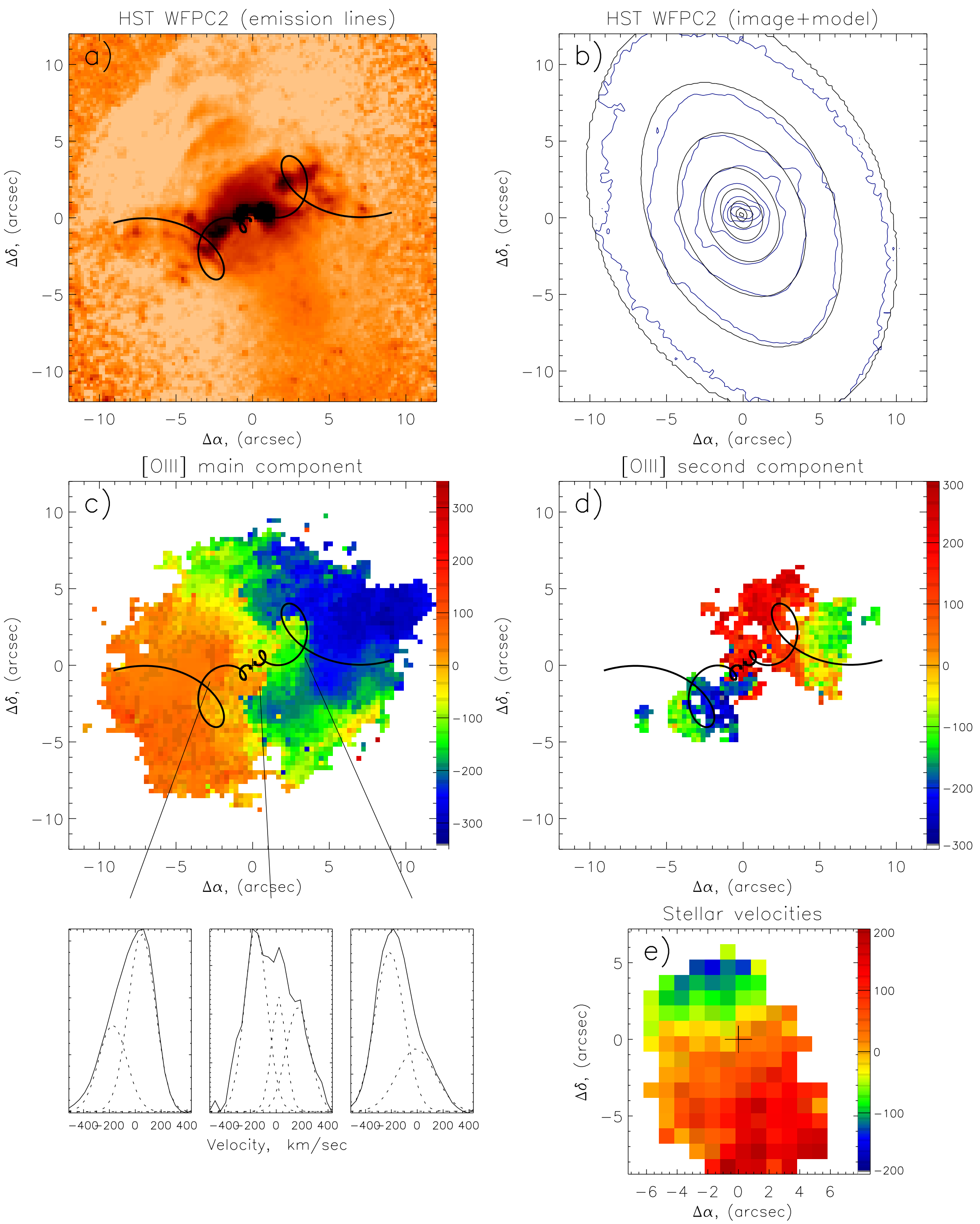

HST WFPC2 (emission lines)
a)
HST WFPC2 (image+model)
b)
[OIII] main component
c)
[OIII] second component
d)
Stellar velocities
e)
Δα, (arcsec)
Δδ, (arcsec)
Velocity, km/sec

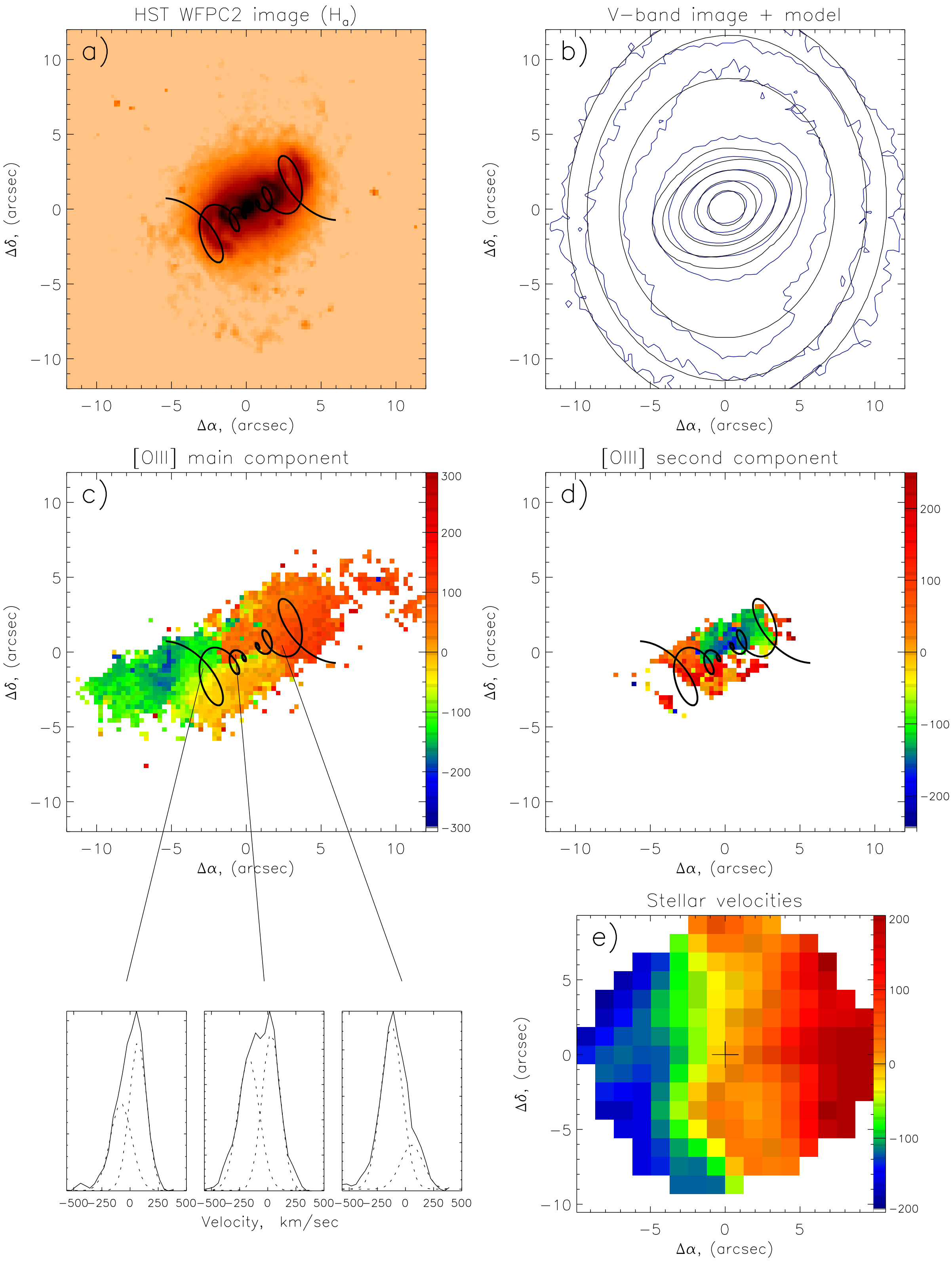

HST WFPC2 image (H_α)
a)
V−band image + model
b)
[OIII] main component
c)
[OIII] second component
d)
Stellar velocities
e)
$\Delta\alpha$, (arcsec)
$\Delta\delta$, (arcsec)
Velocity, km/sec

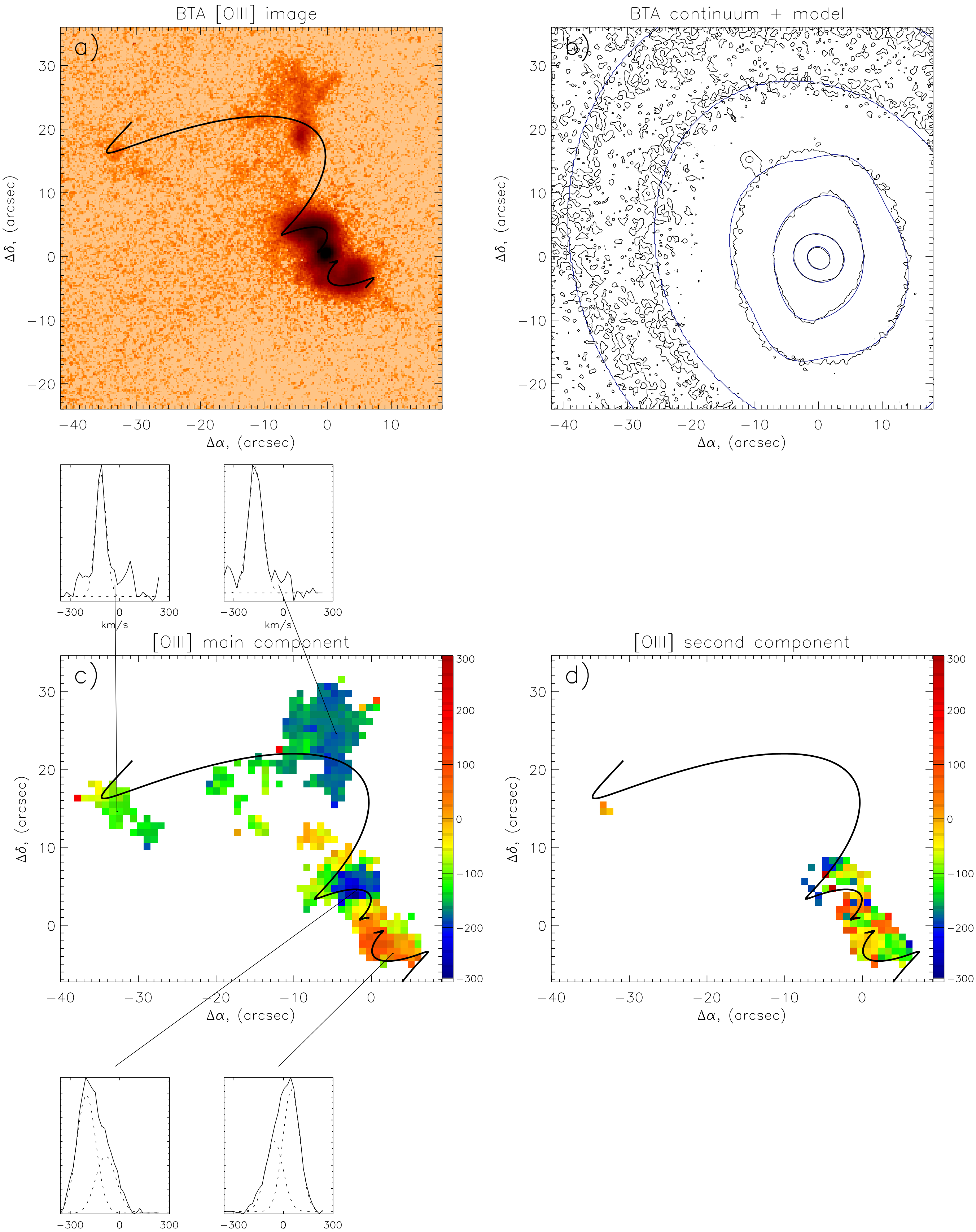

BTA [OIII] image
a)
BTA continuum + model
b)
[OIII] main component
c)
[OIII] second component
d)
Δα, (arcsec)
Δδ, (arcsec)
km/s

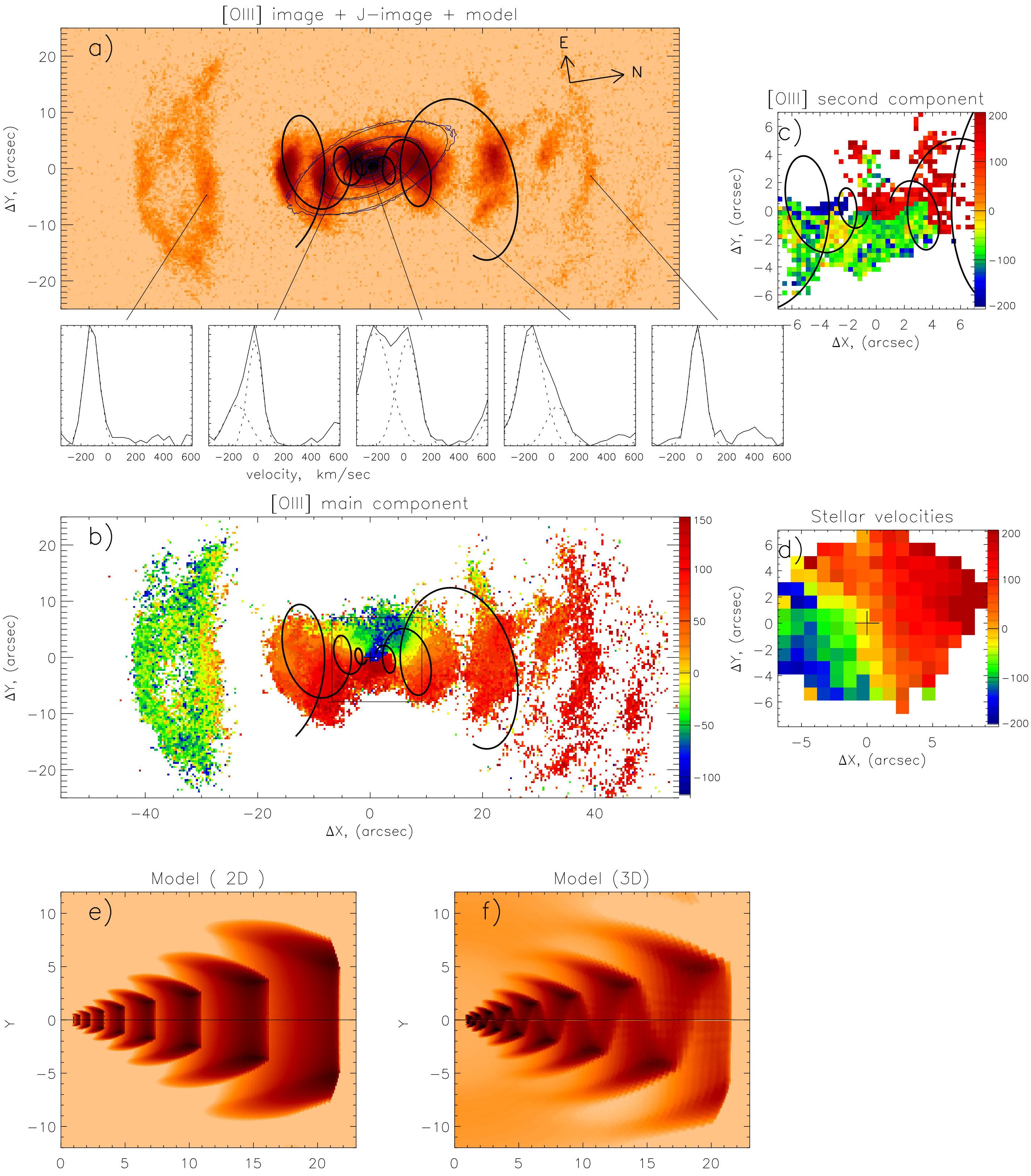
[OIII] image + J-image + model
a)
E
N
ΔY, (arcsec)
velocity, km/sec
[OIII] second component
c)
ΔX, (arcsec)
[OIII] main component
b)
ΔX, (arcsec)
Stellar velocities
d)
Model (2D)
e)
Model (3D)
f)
X
Y